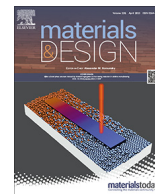




Contents lists available at ScienceDirect

## Materials &amp; Design

journal homepage: [www.elsevier.com/locate/matdes](http://www.elsevier.com/locate/matdes)

## Fluorine free surface modification of tannin-furanic foams by silylation



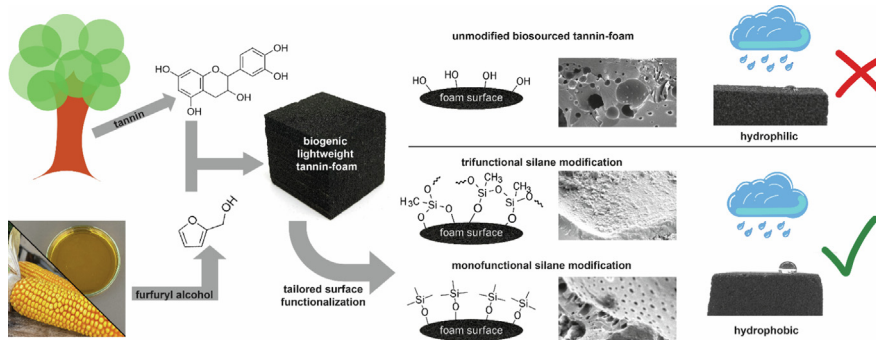
Thomas Sepperer<sup>a,b</sup>, Alexander Petutschnigg<sup>a,b,c</sup>, Ann-Kathrin Koopmann<sup>b,d</sup>,  
Jorge Torres-Rodríguez<sup>b,d</sup>, Primož Šket<sup>e</sup>, Diana E. Bedolla<sup>f,g</sup>, Nicola Hüsing<sup>b,d</sup>, Michael S. Elsaesser<sup>d,\*</sup>

<sup>a</sup> Department of Green Engineering and Circular Design, Salzburg University of Applied Sciences, Markt 136a, 5431 Kuchl, Austria<sup>b</sup> Salzburg Center for Smart Materials, Jakob-Haringer Straße 2a, 5020 Salzburg, Austria<sup>c</sup> Department of Material Sciences and Process Engineering, University of Natural Resources and Life Sciences (BOKU), Konrad Lorenz-Straße 24, 3340 Tulln, Austria<sup>d</sup> Department Chemistry and Physics of Materials, University of Salzburg, Jakob-Haringer Straße 2A, 5020 Salzburg, Austria<sup>e</sup> Slovenian NMR Center, National Institute of Chemistry, 1000 Ljubljana, Slovenia<sup>f</sup> Elettra-Sincrotrone Trieste, S.S. 14 Km 163.5, 34149 Basovizza, Trieste, Italy<sup>g</sup> Area Science Park, Padriciano 99, 34149 Trieste, Italy

## HIGHLIGHTS

- Using fluorinefree organo-silanes allows for effective surface functionalization of biogenic, porous tannin foams.
- Environmentally friendly organo-silanes are able to reduce affinity of tannin-foams to moisture from the environment by 75 %.
- The trifunctional methyltrimethoxysilane can increase the hydrophobicity of biogenic porous materials with a similar effect as perfluoralkoxysilanes.
- By increasing the contact angle to water from 70° to 145°, sustainable tannin-foams could be applied in high humidity areas.
- Modification of tannin-foams allows for tailoring properties and feature new product design possibilities like column chromatography or oil–water separation.

## GRAPHICAL ABSTRACT



## ARTICLE INFO

## Article history:

Received 18 October 2022

Revised 14 April 2023

Accepted 14 April 2023

Available online 20 April 2023

## Keywords:

Biogenic foam

Siloxane grafting

Biosorbent

Fluorine-free hydrophobization

## ABSTRACT

Tannin-furanic foams are a promising and biogenic alternative to oil-based porous materials. Their hydrophilic character, typically indicated by a contact angle to water of 70°, limits some potential applications (for instance outdoor thermal insulation). To overcome this, a post-synthetic surface modification step with different fluorine-free organosilanes at 323 K was investigated with a focus on the final, hydrophobic performance. On the one side, methyltrimethoxysilane, and 3-(chloropropyl)trimethoxysilane, which undergo self-condensation as well as bonding to the hydroxy groups of the tannin polymer, were applied. A modified surface structure and a 25 to 50 % weight increase, depending on the molecular weight of the silylation agent, were observed. Contrary, a mono-functional silane, precisely trimethylchlorosilane, shows only a slight increase in weight, yet also condenses onto the polymer surface without forming a protective surface coating layer. Contact angle measurements using water show an increase from 70° (unmodified) up to 145° for a silane-modified foam. Nuclear magnetic resonance

\* Corresponding author.

E-mail address: [michael.elsaesser@plus.ac.at](mailto:michael.elsaesser@plus.ac.at) (M.S. Elsaesser).<https://doi.org/10.1016/j.matdes.2023.111936>

0264-1275/© 2023 Published by Elsevier Ltd.

This is an open access article under the CC BY-NC-ND license (<http://creativecommons.org/licenses/by-nc-nd/4.0/>).

Porous materials  
Organic–inorganic hybrid

and infrared spectroscopy show the formation of covalent bonds between the silane and the biogenic polymer matrix. The obtained material is less prone to absorb water from a humid atmosphere (reduction of 75 %) and is highly efficient for the removal of non-polar contaminants from water, featuring new possible applications in humid surrounds.

© 2023 Published by Elsevier Ltd. This is an open access article under the CC BY-NC-ND license (<http://creativecommons.org/licenses/by-nc-nd/4.0/>).

## 1. Introduction

Biogenic, polymers and lightweight foams with well-controlled porosity are considered as green future alternatives to conventional, raw oil-based products, in many applications such as thermal or acoustic insulation [1–3], separation media [4,5], semi-conductors [6], fire blocker [7] or medical applications [8]. Tannin-furanic foams are one high-potential candidate, as up to 95 % of the precursors (two main components are plant-derived [9]) are bio-based and frequently abundant at remarkable low costs. The first component is condensed tannin, which can be found in various tree barks, e.g. *Acacia Mimosa*, *Picea Abies*, *Larix Decidua*. While its chemical composition is variable [10], mostly due to the different types and content of flavonoid units (catechin, prorobinetinidin), in general the reactivity is comparable to resorcinol [11]. The extraction from the tree bark is typically done by a simple hot water treatment and reaches a content of pure phenolics between 75 and 90 wt% (with proteins, carbohydrates, and hydrocolloids making up the rest), depending on the source [12,13]. Furfuryl alcohol depicts the second main component, synthesized by catalytic reduction of furfural, a liquid which is obtained by dehydrating pentose-containing biomass (mostly hemicelluloses, sources include corn cobs and wheat straw) [14]. The interaction and polymerization of condensed tannins and furfuryl alcohol in presence of different crosslinkers (formaldehyde, glutaraldehyde, maleic acid anhydride) and various acidic catalysts (sulfuric acid, *p*-toluenesulfonic acid, nitric acid) has been studied intensively over the past years [15–17]. Nowadays, tannin-based foams are optimized regarding their remarkable low thermal conductivity. The materials show competitive properties to commercially available polyurethane or polystyrene foams. Furthermore, additional application areas for tannin-based foams have been explored. These include wastewater treatment with high remediation potential [18,19], its fire retardancy [20], or the addition to cattle manure slurry to mitigate the emission of the greenhouse gas ammonia [21,22].

Many research reports investigate the foam-forming process with a focus on the evaporation of solvents with a low boiling point, such as diethyl ether, pentane, or various alcohols [17,23–26]. Another foaming approach follows the addition of surfactants [27] as well as plasticizers into the non-hardened tannin-furfuryl alcohol mixture with the benefit of enhanced mechanical agitation and finally the creation of a mechanically blown tannin-furanic foam. Based on these protocols, Celzard et al. and Santiago-Medina et al. presented in addition a tannin foam, which was crosslinked with hexamine under alkaline conditions [28,29]. Such foam showed superior mechanical properties (bending strength and compression resistance [30,31]) compared to those made by simple solvent evaporation. However, the hydrophilicity due to the abundant hydroxy groups present in condensed tannins remains one major drawback of all these foams, even when changing the foaming procedure. As a consequence, the absorption of water, either in the form of moisture from the surrounding atmosphere or water droplets after contact [32], results in significantly deteriorating both, the mechanical and thermal properties. Within the last years, only a few attempts to render the tannin-furanic foams more hydrophobic were conducted, including IR treatment, where partial carbonization and thermal degradation of the OH-

groups takes place [33], superficial grafting with environmentally harmful perfluoro-alkyl silanes [34] (formaldehyde containing and hexamine crosslinked foams) or chemical modification of condensed tannins with fatty acids and vegetable oil before use [35].

Organosilanes ( $R_xSi(OR'_{4-x})$  or  $R_xSiCl_{4-x}$  with R being a non-polar organic group such as methyl, propyl, vinyl; R' being methyl or ethyl) have shown reasonable results for hydrophobization [36,37]. 3-(chloropropyl)trimethoxysilane was used in the past to modify starch foams [38] and mesoporous silicon dioxide [39] and showed an increase in hydrophobicity. Methyltrimethoxysilane has been proven useful in case of the synthesis of hydrophobic silica thin films [40], aerogel-glass-fiber composites [41], and silica aerogels in general [42].

In the present study, we focus on the systematic hydrophobization of tannin-furfuryl alcohol- derived foams by using a surface silylation treatment with environmentally friendly and non-toxic silanes. In this approach, free hydroxy groups are reacted with non-polar silane groups to render the material with a pronounced hydrophobic character. For instance, the silylation of silica aerogels is used to allow ambient pressure drying by reducing the condensation of neighboring hydroxy groups with the result of a lower crosslinking degree (less brittleness of the material) [43]. Surface modification by silylation was also successfully presented for organic gels, namely the resorcinol formaldehyde approach [44].

Here, we apply and compare for the first-time fluorine-free mono- and tri-functional organosilanes (trimethylchlorosilane, methyltrimethoxysilane, and 3-(chloropropyl)trimethoxy-silane) concerning their reactivity and hydrophobization performance on formaldehyde-free, biogenic and sustainable tannin-furanic foams. While the mono-functional trimethyl-chlorosilane is only able to react either with the polymers OH-groups or to form dimers that are eluted, the tri-functional silanes can form a 3D network on the polymer's surface. CPTMS in addition allows for additional functionalization in a post-treatment step due to the introduced chlorine functionality [45].

The effective termination of surface hydroxy groups of the biogenic polymer results in a great reduction of the foams affinity to water from the surrounding atmosphere, opening up various new application and design options. For example, the silylated tannin foam is suitable for outdoor applications, where direct contact with water is immanent. Furthermore, due to the greatly reduced water adsorption, the material can be used in product design, where alternating warm/freezing cycles are present (e.g. insulation boxes and other packaging), as not enough moisture is absorbed into the foam that ice would fracture the material's microstructure. Finally, in a proof-of-concept experiment, the separation ability of a water-oil mixture by using such hydrophobized tannin-based foams is presented, proofing that the material can be applied as a biogenic adsorbent for oil contamination on water after e.g. oil tanker damages.

## 2. Experimental: Material and methods

### 2.1. Chemicals and reagents

Industrial mimosa tannin extract Fintan OP was kindly provided by SilvaTeam (San Michele Mondevi, Italy). Furfuryl alcohol

(>99.8 %) was acquired from IFC (Geel, Belgium). Polysorbate 80 was purchased from Carl Roth (Karlsruhe, Germany). Methyltrimethoxysilane (98 %), 3-(chloropropyl)trimethoxysilane (98 %) and trimethylchlorosilane (99 %) were purchased from VWR (Darmstadt, Germany). All other chemicals (VWR) were used without further purification.

## 2.2. Foam preparation

Tannin-furanic foams were synthesized as described previously [30] using a bench-top dissolver for rapid agitation (Dispermat-LC, VMA-Getzmann, Germany). In short, mimosa tannin (10 g) was mixed with furfuryl alcohol (6.2 g), water (3 g), diethylene glycol (3 g), and polysorbate 80 (1.6 g) and homogenized for 5 min at 200 rpm. Afterward, the stirring speed was increased to 1000 rpm, diluted sulphuric acid (2 M, 4 g) was added and stirred to the final volume for approx. 15–20 min. The foam was then transferred into a Teflon-covered mold and hardened in an oven for 30 min at 333 K. Drying was performed for another 24 h at 333 K after removing the foam from the mold. Finally, the foam was cut into samples of  $13 \times 13 \times 40 \text{ mm}^3$  and dried before further use.

## 2.3. Hydrophobization

Surface modification of the dried foam pieces was conducted using different amounts (5, 10, and 20 vol%) of three different organosilanes (trimethylchlorosilane (TMCS), methyltrimethoxysilane (MTMS), and 3-(chloropropyl)trimethoxysilane (CPTMS)) in heptane. The foams were immersed in the silane/heptane solution in a round bottom flask and a vacuum of 700 mbar was applied for 5 min to remove the air trapped inside the foam's cavities. Subsequently, the vacuum was removed allowing the silane-heptane solution to fill the voids. This process was repeated once more. Afterward, the immersed foam was heated to 323 K for 24 h. Samples were then removed from the solution and washed with heptane to remove unreacted silanes and dried in a vacuum oven at 333 K for 24 h. The weight of the samples was recorded before and after silylation to calculate the effective loading. Nomenclature was set as follows: Abbreviation of the silane and a subscript number indicating the concentration (e.g. MTMS<sub>10</sub> means methyltrimethoxysilane modified foam, where 10 vol% of silanes were used in the silylation solution, a complete list of sample nomenclature can be found in Table S1.). To eliminate the influence of the heptane washing on the results, the reference material was also treated in heptane at 323 K for 24 h.

## 2.4. Characterization of the modified material

**Weight gain (WG):** The weight of the dried foam pieces was recorded before modification and after the complete silylation treatment and drying. Weight gain was calculated according to equation (1), where  $m_m$  is the weight of the modified foam and  $m_u$  is the weight of the unmodified starting material.

$$WG = \frac{m_m - m_u}{m_u} \cdot 100[\%] \quad (1)$$

**Thermo gravimetric analysis (TGA):** Weight loss as a function of time and temperature was determined using a Netzsch STA 449 F3 Jupiter instrument (Selb, Germany). The sample was heated at a rate of  $10 \text{ K min}^{-1}$  to 1273 K in a synthetic air atmosphere.

**Scanning electron microscopy (SEM)** imaging was done using a Zeiss Ultra Plus field emission scanning electron microscope equipped with an annular backscatter electron detector (Carl Zeiss AG, Oberkochen, Germany). The acceleration voltage was set to

5 kV and the working distance was adjusted between 4 and 6 mm. Before the imaging, the samples were coated with a thin layer of gold using a sputter coater with a current of 40 mA and a coating time of 90 s.

**Scanning transmission electron microscopy (STEM)** images, such as the secondary and back-scattered electron or high-angle annular dark-field (HAADF) images, displaying z-contrast were acquired using a cold field emission JEOL F200 STEM/TEM operated at 200 kV equipped with a large windowless JEOL Centurio EDX detector ( $100 \text{ mm}^2$ , 0.97 srad, energy resolution < 133 eV). EDX maps were recorded with a typical beam current of 0.1 nA and a beam diameter of 0.16 nm for 15 min. The maps were obtained by signal integration of counts over the Si K $\alpha$  transition line for Si (integration: 1.63–1.89 keV), O K $\alpha$  line for O (integration: 0.46–0.59 keV), and C K $\alpha$  line for C (integration: 0.21–0.34 keV).

**Attenuated total reflectance Fourier-transform infrared (ATR-FT-IR)** spectra were collected using a Perkin-Elmer (Perkin-Elmer, Waltham, USA) Frontier FT-IR spectrometer, equipped with an ATR Miracle accessory. 32 scans were performed for each sample, at a resolution of  $4 \text{ cm}^{-1}$ , in the range  $4000\text{--}600 \text{ cm}^{-1}$ , and Bio Rad KnowItAll (BioRad, California, USA) software was used for normalizing and averaging.

**FT-IR Imaging** on thin slices of foams was done using a 64 pixels  $\times$  64 pixels Focal Plane Array over an area of  $150 \mu\text{m} \times 150 \mu\text{m}$  with a spatial resolution of about  $2.6 \mu\text{m} \times 2.6 \mu\text{m}$ . A Vis-IR microscope Bruker Hyperion 3000 with a 15x objective/condenser coupled to a Bruker Vertex 70v was used to accumulate 128 scans for each background and sample at a spectral resolution of  $4 \text{ cm}^{-1}$  in the range of  $4000\text{--}850 \text{ cm}^{-1}$ . All spectra were corrected for water vapor and CO<sub>2</sub> contribution using the OPUS software.

**Solid-state <sup>13</sup>C CP MAS, <sup>29</sup>Si CP MAS, and <sup>29</sup>Si MAS NMR** experiments were performed on an Agilent Technologies NMR System 600 MHz NMR spectrometer equipped with a 3.2 mm NB Double Resonance HX MAS Solids Probe. The sample spinning frequency was 20 kHz. The <sup>13</sup>C CP MAS NMR experiments consisted of excitation of protons with p/2 pulse of 2.6  $\mu\text{s}$ , CP block of 5 ms, and signal acquisition with high-power proton decoupling. A total of ca. 15,000 to 27,000 scans were accumulated with the repetition delay of 3 s. The chemical shifts were referenced externally using adamantane. The <sup>29</sup>Si CP MAS NMR experiments consisted of excitation of protons with p/2 pulse of 2.85  $\mu\text{s}$ , CP block of 5 ms, and signal acquisition with high-power proton decoupling. A total of ca. 9000 to 14,000 scans were accumulated with the repetition delay of 2 s. The <sup>29</sup>Si MAS NMR spectra were acquired using one pulse sequence with high-power proton decoupling during acquisition. A total of ca. 700 to 1800 scans were accumulated with a repetition delay of 60 s. The <sup>29</sup>Si-CP-MAS and <sup>29</sup>Si MAS NMR spectra were externally referenced using DSS ( $\delta$  1.53 ppm).

**Contact angle (CA)** measurements were performed using a Krüss DSA1 (Krüss, Hamburg, Germany) and the three standard liquids (water, ethylene glycol, and diiodomethane). A droplet of 5  $\mu\text{L}$  was placed on top of the material and the contact angle was measured every 10 s for a period of 100 s. A total of three measurements were done for each liquid and surface on independent places on the samples. Contact angles were calculated using Krüss Software. **Surface energy (SE)** was calculated from the contact angle data according to the method of Owens, Wendt, Rabel, and Kaelble (OWRK) [46].

**Vapor saturation:** To evaluate the equilibrium moisture content in a standardized climate, samples were first dried at 376 K for 24 h and their weight was recorded. Afterward, they were placed in a climate chamber (Binder, Germany) at a temperature of 296 K and relative humidity of 65 %. Weight gain was recorded after 1, 2, 3, and 6 days.

### 3. Results and discussion

#### 3.1. Hydrophobization of tannin-furanic foams by silylation

Fig. 1 shows a general overview of the synthesis procedure and subsequent surface modification as applied in this work. First, a tannin foam monolith is prepared by a classical foaming protocol based on tannin, furfuryl alcohol, and Polysorbate 80 in water, as described in our previous study [30]. Briefly, tannin was mixed with furfuryl alcohol, water, and surfactants and homogenized for 5 min before agitation speed was increased and the acidic catalyst is added. When the desired foam volume is reached, the blend is transferred into a mold and polymerized in a convection oven. After curing the foam and cutting it to an appropriate size, the hydrophobization was carried out in various silylation solutions. Thereafter, the surface-modified foams were rinsed and dried completely in a vacuum oven, yielding the hydrophobic, biogenic foam.

The macroscopic, unmodified tannin-furanic foam monolith can be seen in Fig. 2A, its corresponding micro-morphology is depicted by an SEM micrograph in Fig. 2B, and with higher magnification (3000x) in Fig. 2C. A typical foam-like structure represented by spherical voids with a size of 200–500  $\mu\text{m}$  interconnected by porous cell walls is obviously present. Thus, the presence of  $\mu\text{m}$ -sized smaller pores in the solid fraction allows accessibility and mass transport between the main foam bubbles.

Surface hydrophobization was now performed by immersing the aforementioned tannin-furanic foams, cut into  $13 \times 13 \times 40 \text{ mm}^3$  sized pieces, into one silane solution with various concentrations (either trimethylchlorosilane (TMCS), methyltrimethoxysilane (MTMS) and 3-(chloropropyl)trimethoxysilane (CPTMS) at a concentration of 5, 10 and 20 vol% in heptane). The silylation reaction was stopped after 24 h and the corresponding, surface-treated monolith was obtained after drying. An exemplary SEM image in Fig. 2D shows the surface of the inner cell wall of an  $\text{MTMS}_{20}$  mod-

ified foam, and an SEM image in Fig. 2E the cell wall of  $\text{CPTMS}_{20}$  modified foam. Both show a change in the surface structure due to the silane modification: the original foam wall is coated and smaller pores are blocked. By contrast, the cell wall of a  $\text{TMCS}_{20}$  modified material (Fig. 2F), shows no differences from the unmodified foam. CPTMS and MTMS both have three reactive sites allowing the potential formation of three-dimensional networks and coating on the surface of the tannin-furanic substrate. TMCS on the other hand only contains one condensable group and therefore is only able to form dimers on the tannin-furanic foam's surface. This seems to be causing the differences in surface morphology.

#### 3.2. Chemical and physical analysis of silylated tannin-furanic foams

The weight gain for all samples is shown in Fig. 3. As expected, CPTMS results in the highest weight increase, with around 50 % of the initial weight at each of the three concentrations. When modifying tannin-furanic foams with MTMS, a concentration of 5 % in heptane results in the highest weight gain with 29 % ( $\text{MTMS}_5$ ). With increasing silane concentration, the loading decreases to only around 19 % weight gain for  $\text{MTMS}_{20}$ . Apparently, only a distinct amount of MTMS can be chemically bonded and residual molecules are washed out during purification (similar to CPTMS). Using TMCS as silylation agent results in the lowest weight gain with a maximum of 5 %, independent from the applied concentration of the silylation agent.

The results of the remaining mass after heating the silylated foams to 1273 K (TGA) under synthetic air are also presented in Fig. 3. It can be assumed that the ash of the modified foams consists predominantly of  $\text{SiO}_2$  and therefore further insights into the degree of silylation can be derived. The unmodified foam has a remaining mass of roughly 4 % which can for the most part be attributed to chains of (poly)furfuryl alcohol forming in the

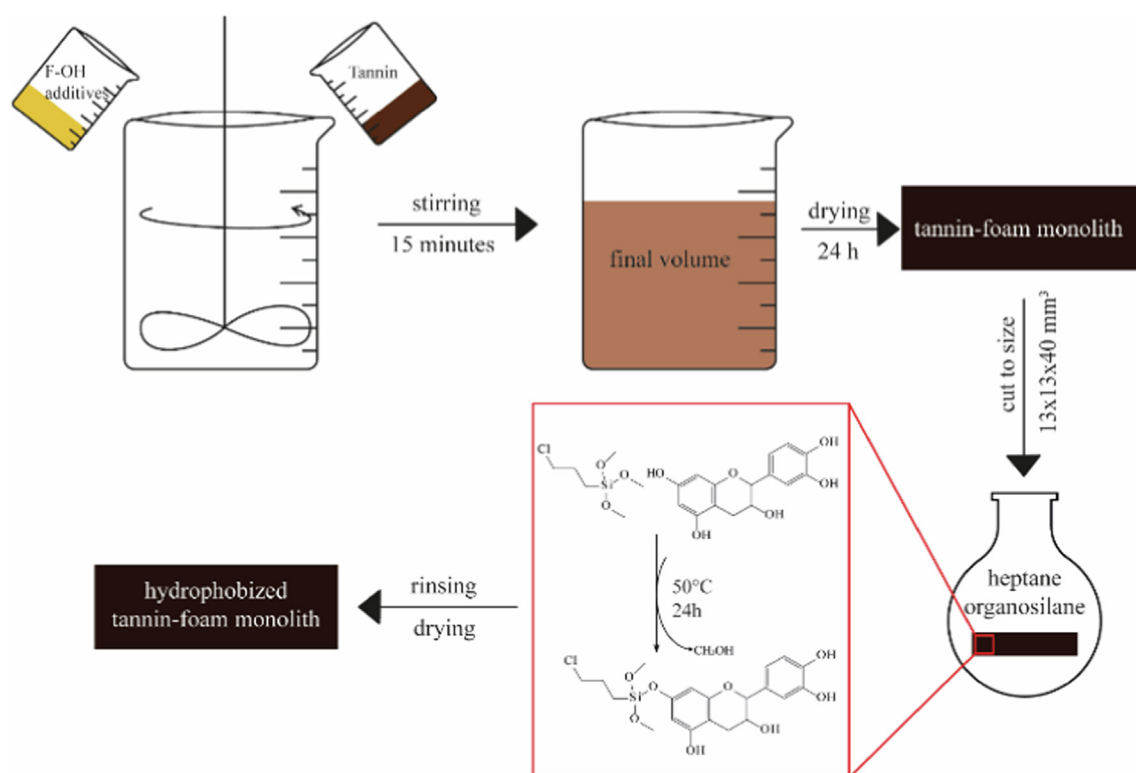
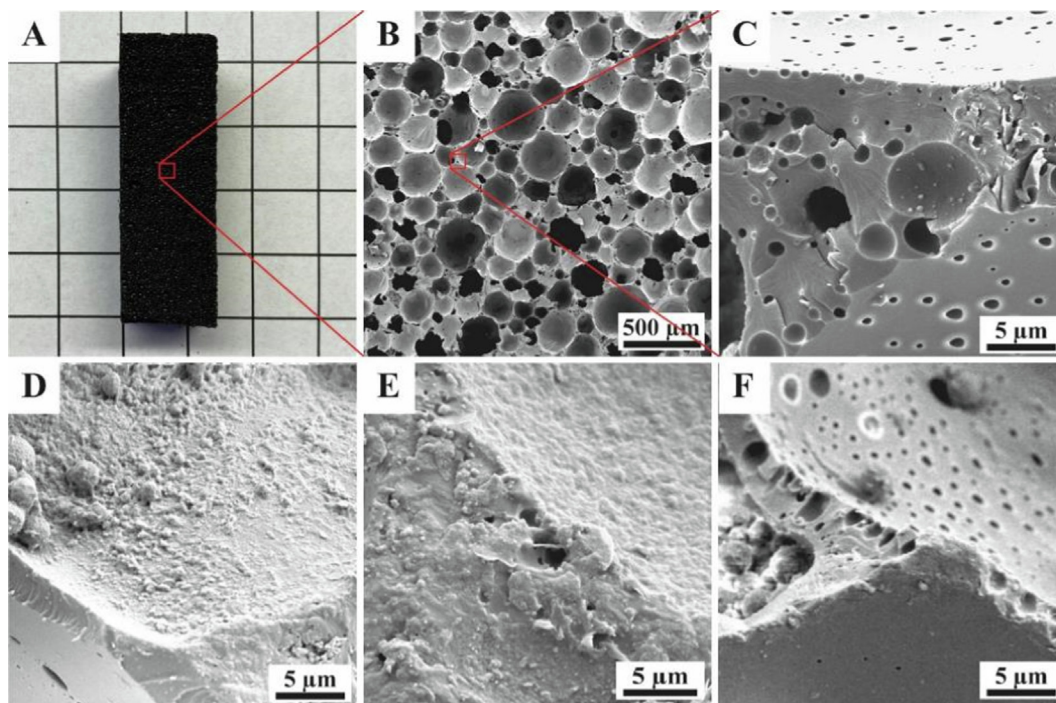
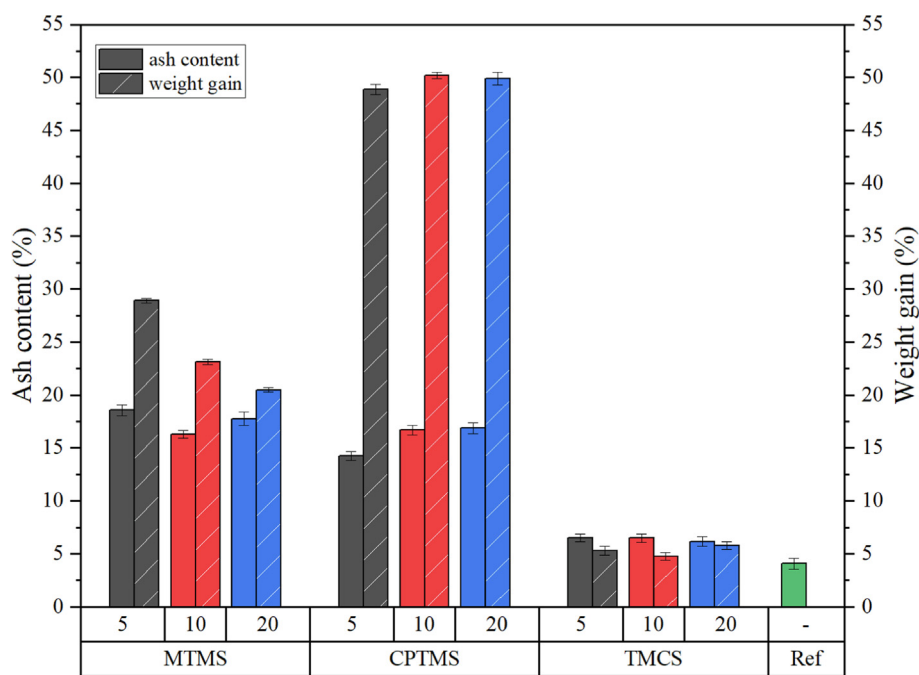


Fig. 1. Foam synthesis and schematic representation of the surface modification process. (with a suggested chemical reaction of the surface silylation treatment).



**Fig. 2.** Unmodified tannin-foam monolith on a 1 cm<sup>2</sup> grid (A), SEM images (B–F) from unmodified foams (B, C), and from silylated foams with MTMS<sub>20</sub> (D), CPTMS<sub>20</sub> (E) and TMCS<sub>20</sub> (F).



**Fig. 3.** Weight gain and ash content of the functionalized foams. Unmodified foam included as reference (Ref).

tannin-furanic polymer. Similar materials are reported in the literature to have an ash content between 20 and 40 % after heating to 1273 K in synthetic air [47,48] and also mimosa tannin, which has an ash content of around 2.5 % consisting mostly of calcium-, sodium- and magnesium-oxide [49]. Trimethylchlorosilane-modified foams show only a small increase in inorganic remaining mass. For all three different amounts of TMCS only around 6 % remain as ash after heating. As only one condensable site is present

in TMCS, this result could be expected. TMCS therefore can only react directly with the polymer's surface and not create three-dimensional networks coating the tannin-furanic foam. Despite the higher weight gain when using CPTMS as modifying agent compared to MTMS, the inorganic remains are in a similar range of 15–17 %. The heavier chloro-propyl tail (77 Da) of CPTMS compared to the methyl group (15 Da) of MTMS that are thermally degraded during heating explains the difference between initial

weight gain and similarity in ash content. This indicates that both, CPTMS and MTMS are reacting approximately to the same extent with the tannin-furanic polymer.

To evaluate changes in the physical properties of the foam surfaces after silylation treatment, contact angle measurement experiments were performed.

Side-view pictures from the water droplet acquired during contact angle measurements of the pristine and with 5 vol% silane treated foams are displayed in Fig. 4. The exact values for contact angles with each liquid including the standard deviation are listed in Table S2. Fig. 4A shows the case for the unmodified foam, for which the water droplet quickly loses its shape resulting in a contact angle of around  $70^\circ$ , indicating a hydrophilic character [50]. The CPTMS<sub>5</sub> (Fig. 4B) and MTMS<sub>5</sub> (Fig. 4C) modified foams on the other hand both retain the drop shape at an angle of  $128^\circ$  and  $135^\circ$ , respectively, which confirms them clearly as hydrophobic [50]. The TMCS<sub>5</sub> (Fig. 4D) modified foam results also in a contact angle to water of roughly  $115^\circ$ , which also counts as hydrophobic.

The highest hydrophobization effects are obtained for CPTMS and MTMS modified foams with a concentration of 10 vol% silane in the silylation solution (CPTMS<sub>10</sub> and MTMS<sub>10</sub>). They show contact angle values to water of  $143^\circ$  and  $145^\circ$ , a non-polar fraction to diiodomethane of  $100^\circ$  and  $112^\circ$ , and against ethylene glycol at  $146^\circ$  and  $137^\circ$ , respectively.

As TMCS selectively reacts with only one OH-group on the polymer surface, the degree of loading is not comparable to CPTMS and MTMS. Nevertheless, hydrophobization is very efficient indicating a successful surface modification. When using trimethylchlorosilane as a silylation agent, a high applied concentration of 20 vol% shows the best results with a contact angle value of  $131^\circ$ ,  $91^\circ$ , and  $57^\circ$  for water, diiodomethane, and ethylene glycol, respectively. Similar and higher values were achieved for the modification of stone surfaces with siloxane emulsions where contact angles to water, ethylene glycol and dodecane of  $162^\circ$ ,  $159^\circ$  and  $125^\circ$  were reported [51].

Using fluorinated silanes to modify the tannin-polymer surface, an increase in the contact angle for water and ethylene glycol in a similar range ( $130 - 140^\circ$ ) was observed [34]. When modifying the tannins with vegetable oil before foam synthesis, the contact angle

to water only increases to around  $128^\circ$  while for ethylene glycol it changes to  $93^\circ$  [35].

To get further insights into the foam surface hydrophobization performance, surface energies  $\gamma$  (total as well as disperse and polar fraction) were calculated according to the model of Owens, Wendt, Rabel, and Kaelble (OWRK) [46] and listed in Table S1. The corresponding wetting envelopes created from the surface energy data are shown in Fig. 5 for the three silanes used. For comparison, the wetting envelope for the unmodified reference foam is included in each graph. For all modifications and all applied concentrations, a decrease in total surface energy  $\gamma$  was observed as seen by the smaller area under the wetting envelopes. Especially the polar part  $\gamma^p$  disappears almost completely for all modifications. It reaches a minimum of  $0.06 \text{ mN m}^{-1}$  for MTMS<sub>5</sub> compared to  $5.12 \text{ mN m}^{-1}$  for the reference material. The disperse portion of the surface energy  $\gamma^d$  decreases also for all modifications with the most promising results for MTMS<sub>10</sub> where it is reduced to roughly a tenth of the original value. When using TMCS as a hydrophobization agent, a concentration of 20 vol% lead to the best results, with a reduction of around 50 % compared to the unmodified material. CPTMS<sub>5</sub> shows only a poor hydrophobization improvement.

A drastic reduction of surface energy (from 58 to  $5.4 \text{ mN m}^{-1}$ ), especially for the polar part, was also obtained by Delgado-Sánchez et al. for fluorinated silanes and vinyltrimethoxysilane when applied to chemically expanded tannin foams containing formaldehyde [34]. Other than silylation, oil-grafting of tannins only altered the polar proportion of the surface energy, not the dispersive one [35].

Solid state NMR serves as a powerful method to prove the structure and chemical composition after silylation treatment. Qualitative  $^{13}\text{C}$  CP MAS NMR and  $^{29}\text{Si}$  MAS NMR (allowing quantitative statements) spectra for reference CPTMS<sub>10</sub> and MTMS<sub>10</sub> foams are shown in Fig. 6A and B, respectively.  $^{29}\text{Si}$  CP MAS NMR spectra are shown in Fig. S2. A detailed assignment of the  $^{13}\text{C}$  signals for the reference foams can be found in the literature [30,52]. For CPTMS<sub>10</sub>, three additional peaks can be observed in the carbon NMR spectrum with a chemical shift of 48, 27, and 11 ppm, and all can be assigned to the chloropropyl group of the silane. The signal at 48 ppm, which can be assigned to the methoxy carbon, dis-

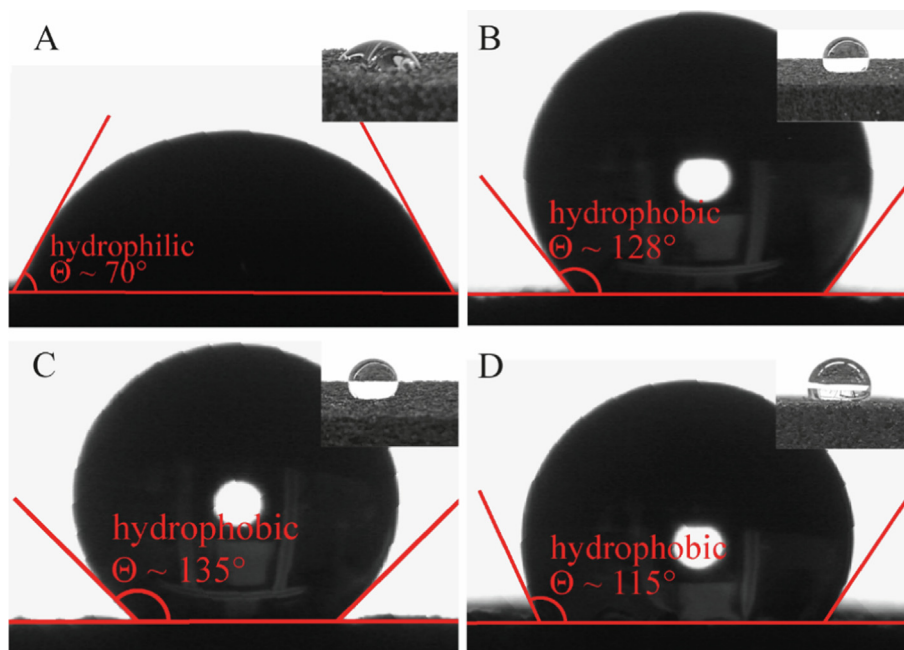


Fig. 4. Contact angle measurements with water and an unmodified foam (A), or silylated foam with CPTMS<sub>5</sub> (B), MTMS<sub>5</sub> (C), and TMCS<sub>5</sub> (D).

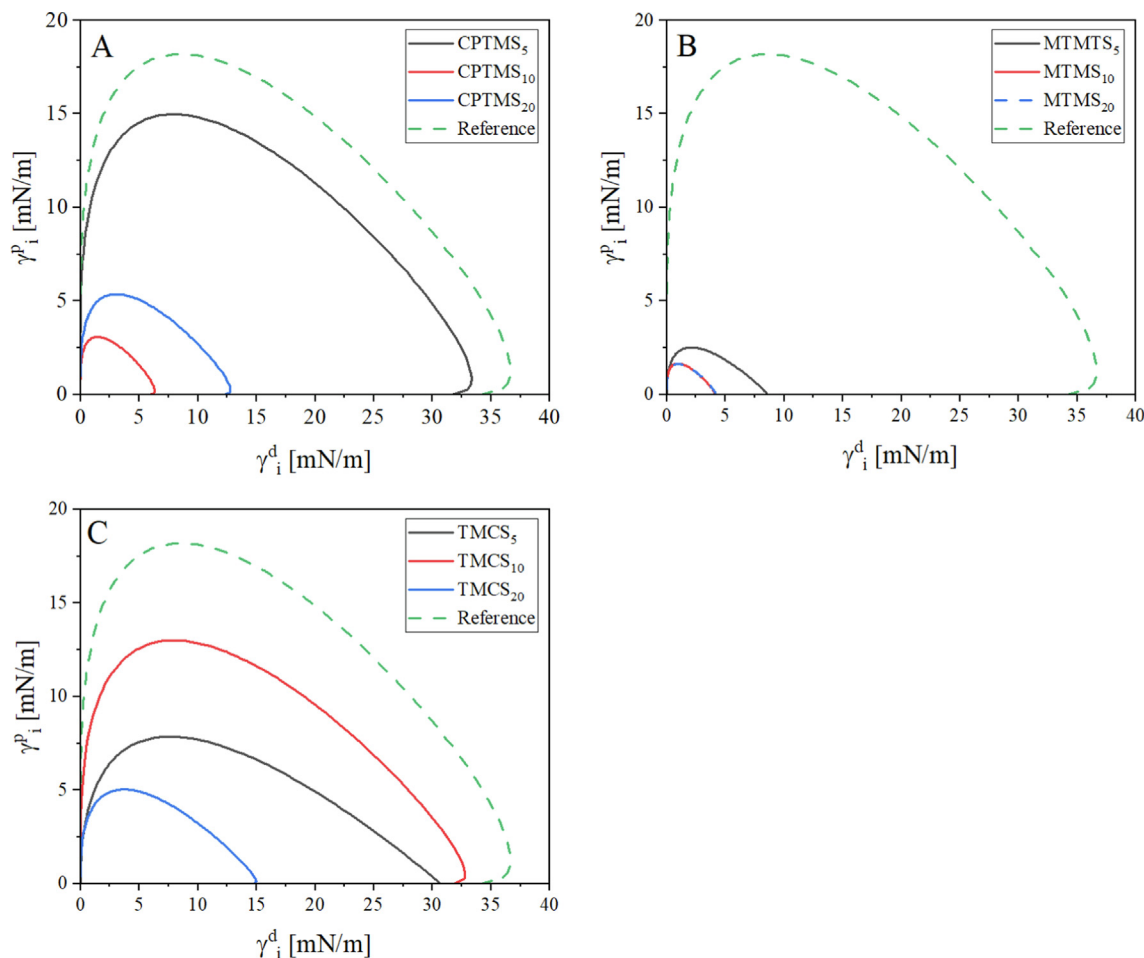


Fig. 5. Wetting envelopes for CPMTS (A), MTMS (B) and TMCS (C) modified foams. Unmodified foam is included as a reference in each.

appears almost completely in the spectrum of MTMS<sub>10</sub> modified foam, indicating a high level of hydrolysis and rather complete condensation to either the polymer surface or other silane molecules that are attached to the tannin polymer structure. For MTMS the signal at  $-3$  ppm clearly indicates the presence of  $\text{CH}_3\text{-Si}$  moieties in the material proving the successful modification. For TMCS this signal is not observed. This can be due to the expected low concentration of silicon-bound methyl groups in the sample.

Fig. 6B shows the  $^{29}\text{Si}$  MAS NMR for the modified material and the reference. Peaks are labeled with  $\text{T}^n$  where  $n$  represents the number of siloxane bonds [53]. For CPTMS<sub>10</sub> modified foams, two distinct peaks at  $-67.2$  ppm and  $-58.8$  ppm (with an additional shoulder at  $-54.7$  ppm) are present corresponding to  $\text{T}^3$  and  $\text{T}^2$  moieties, respectively [38]. In the MTMS<sub>10</sub> treated foam, the chemical shifts for  $\text{T}^3$  and  $\text{T}^2$  are found in a similar shift range ( $-65.6$  ppm and  $-56.4$  ppm, respectively) with a broadening of the  $\text{T}^2$  peak into the  $\text{T}^1$  region. A schematic representation of  $\text{T}^1$ ,  $\text{T}^2$ , and  $\text{T}^3$  siloxane bonds is shown in panel C of Fig. 6. NMR data suggests more self-condensation of all three reactive sites of the alkoxy silane for MTMS compared to CPTMS due to the lower intensity of the  $\text{T}^2$  signal. TMCS<sub>10</sub> was intentionally left out of the figure, as neither T, Q nor D signals are expected. Additionally, also the expected M peak was not observed.

One dimensional FT-IR spectroscopy (Fig. 6D) of the modified foams shows an additional signal for MTMS<sub>5</sub> at  $1270\text{ cm}^{-1}$  corresponding to C–O stretching vibrations of aromatic esters or ethers, indicating a reaction between the alkoxy silane and the hydroxy group of the tannin. The new peak at  $775\text{ cm}^{-1}$  can be attributed

to a Si–C stretching vibration in the silylated polymer. A broadening and also less defined peaks in the aromatic alcohol region between  $1200$  and  $1000\text{ cm}^{-1}$  further confirm the reduction of aromatic OH by condensation with the silane [54–56]. The same peaks and changes in the spectrum can be observed for CPTMS<sub>5</sub>. In the same area, the Si–O–Si stretching vibration takes place, as seen for both, CPTMS and MTMS with a more defined peak at  $1020\text{ cm}^{-1}$ . Furthermore, new peaks at  $1235\text{ cm}^{-1}$  and  $695\text{ cm}^{-1}$ , correspond to aromatic ether/ester and C–Cl, respectively. In the spectrum of TMCS<sub>5</sub>, no changes compared to the spectrum of the original material can be observed.

As a homogeneous surface treatment is considered with high priority, we analyzed exemplarily a sample also by two-dimensional infrared spectroscopy using a focal plane array detector. Therefore, a slice with a thickness of  $30\text{ }\mu\text{m}$  of CPTMS<sub>10</sub> was prepared and an image of the sample section, which is investigated, is shown in Fig. 7A. By integrating spectral regions, three distinct areas along the cross-section were created. (i)  $1760\text{--}1560\text{ cm}^{-1}$  a region typical for tannin-furanic polymer (Fig. 7B, red), (ii)  $3030\text{--}2824\text{ cm}^{-1}$  representing aliphatic signals (Fig. 7C, green), and (iii)  $1212\text{--}940\text{ cm}^{-1}$  (Fig. 7D, blue) a region where both, silica and tannin-furanic polymer have high intensities, yet the Si–O–Si vibration should be dominant. Furthermore, three selected spectra of the foam slice at three different regions are presented: (i) a junction, where the cell walls touch (Fig. 7F, purple), (ii) the surface of the cell wall (Fig. 7F, green), and (iii) an intermediate region between junction and wall (Fig. 7F, blue). The junction position shows high intensities in the region of  $1760\text{--}1570\text{ cm}^{-1}$

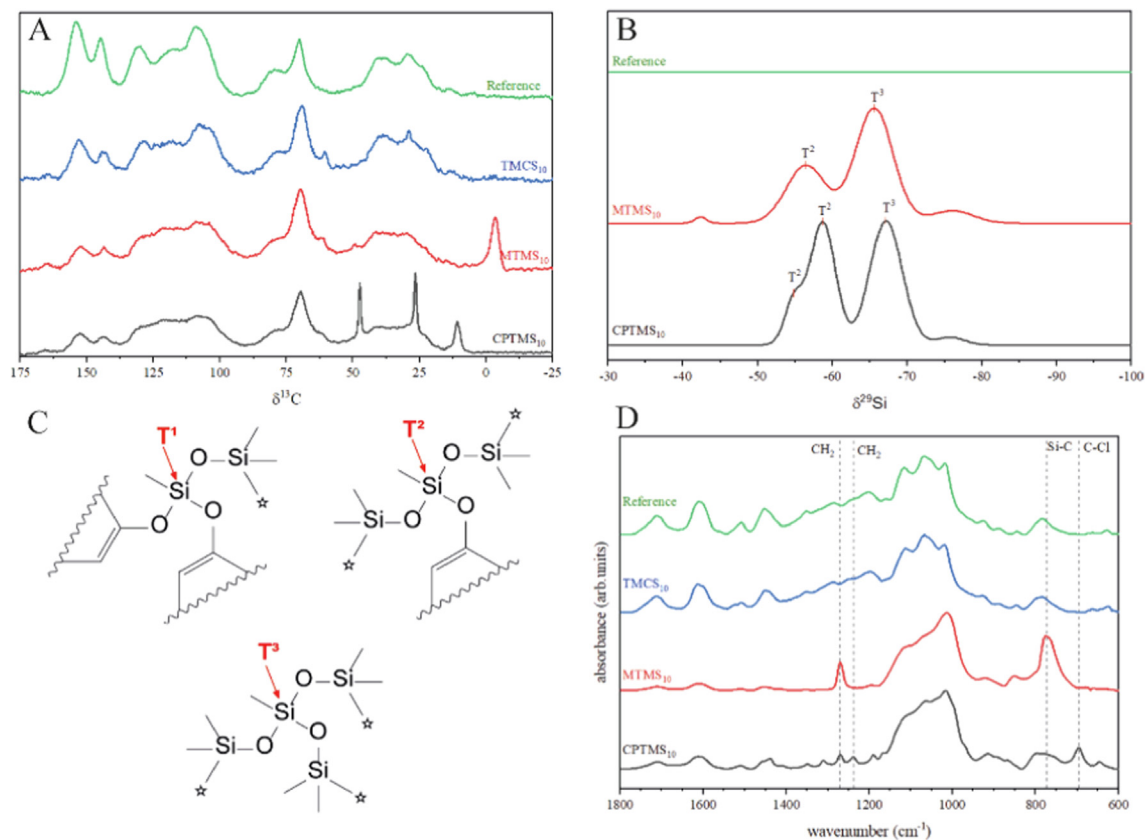


Fig. 6.  $^{13}\text{C}$  CP MAS NMR (A),  $^{29}\text{Si}$  MAS NMR (B), schematic representation of  $\text{T}^1$ ,  $\text{T}^2$ , and  $\text{T}^3$  siloxane bonds (C), and normalized 1D FT-IR spectra (D).

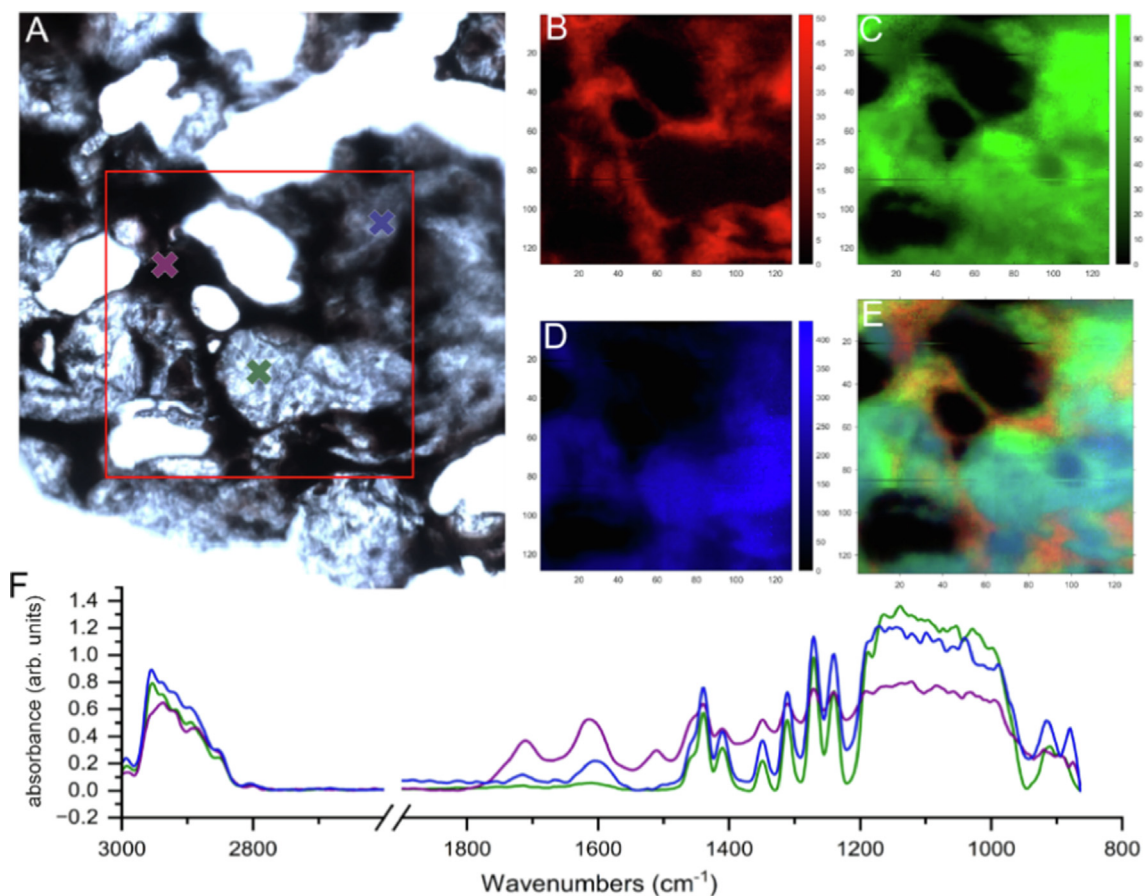


Fig. 7. Micrograph of the CPTMS<sub>10</sub> slice used for imaging (A), 2D FT-IR imaging (B–D) from CPTMS<sub>10</sub> foam: (B) integral 1760–1560  $\text{cm}^{-1}$  (B), integral 3030–2824  $\text{cm}^{-1}$  (C), integral 1212–940  $\text{cm}^{-1}$  (D), RGB merge of the three integration regions (E). Single FT-IR spectra corresponding to the points marked in (A) in purple, blue and green (F).

clearly indicating the dominance of the tannin-furanic polymer, this can be observed further in the corresponding imaging (Fig. 7B), where the highest intensities are seen for regions with predominantly knots. These regions also show less intense signals in the Si–O–Si region (Fig. 7D and E). The cell walls (marked with a green cross in Fig. 7A) show a high intensity in the region of 1212–940  $\text{cm}^{-1}$  and almost no signal in the 1755–1568  $\text{cm}^{-1}$  region, indicating that the organosilanes form a protective layer onto the tannin-furanic polymer. This can also be seen in the SEM micrographs in Fig. 2E, where a change in surface morphology is visible. Results of the FT-IR imaging show that surface modification with CPTMS can be easily done, yet a complete penetration of the whole polymer is not possible with the experimental conditions applied. FT-IR imaging for MTMS-modified foams can be seen in Fig. S3. The ratio of Si/Tannin was calculated and is illustrated in Fig. S4 for both, CPTMS and MTMS modified tannin-furanic foam slices.

For elemental mapping, scanning transmission electron microscopy images confirm the presence of silicon on the tannin-furanic polymer after silylation treatment as seen in Fig. 8. For CPTMS and MTMS (Fig. 8A and B) higher concentrations of silicon within the polymer are present (represented in blue) as already confirmed by NMR, FT-IR and TGA. For TMCS-modified foams, only small amounts of silicon are detected, which could explain the slight increase in inorganic remaining mass after heating (Fig. 3) and further supports the explanation that only a selective modification of the tannins' surface hydroxy groups takes place.

### 3.3. Testing of hydrophobized tannin foams under natural conditions

Storing modified foam monoliths in a humid climate establishes the equilibrium moisture content (EMC). For all samples, the EMC is considered to be reached after six days, as no more changes in weight are observed between two measurements between the interval of three and six days. Fig. 9 shows the weight gain for each modified foam within the six days period. The unmodified foam absorbs around 22 wt% water within three days. Independent from the used concentration, modification with TMCS results in a reduction of the EMC to 12 wt%, where the first 7 wt% are absorbed within one day, after two days of exposure to a humid environment only small changes are recorded. Methyltrimethoxysilane modification leads to a reduction of EMC to 6 wt% at all concentrations used. Interestingly, after one day almost no changes in weight gain are recorded, indicating that all the moisture is absorbed within the first day of exposure. CPTMS<sub>5</sub> shows a behavior similar to the MTMS modified material, whereas CPTMS<sub>10</sub> and CPTMS<sub>20</sub> both only absorb 4.8 wt% after six days. Furthermore, absorption in CPTMS<sub>20</sub> is much slower compared to the other materials, as after one day only 2.8 wt% weight gain is recorded. Mitigation of

the overall equivalent moisture content of the silane-modified foams suggests that the silylation of tannin-derived hydroxy groups does happen throughout the monolith and not only on the outer-most surface regions as it happens by superficial modification methods such as IR irradiation or silylation without a proper vacuum impregnation cycle to ensure complete saturation of the monolith with a silylating solution. MTMS and CPTMS modified foams show water absorption in a humid atmosphere comparable to commercial polyurethane [57] or polystyrene [58] foams, which opens up new possibilities for application.

Effective separation of water–oil mixtures depicts nowadays a very important industrial field concerning huge amounts of wastewater and its environmental compatibility. Hydrophobized biogenic foams could be promising future materials. We designed a simple proof-of-concept experiment, to show the ability to remove non-polar contamination from water: we tested qualitatively by pipetting 2 mL of toluene or heptane (red-colored) onto the water and swirling around a piece of the modified foam in a beaker. A picture series showing the progress of the procedure using toluene and MTMS<sub>20</sub> foam can be seen in Fig. 10. Already after a few seconds, the red-colored toluene layer is absorbed completely onto the modified foam. Additionally, a fine-grounded, hydrophobized foam was poured into a test tube filled with water and toluene/heptane and shaken vigorously using a vortex stirrer. The modified foam powder absorbs the non-polar liquid and aggregates into a lump that could easily be removed from the water.

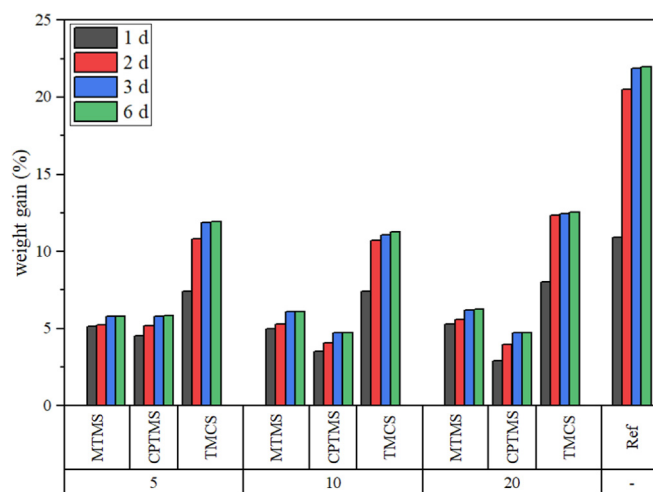


Fig. 9. Weight gain through vapor saturation for all silylated tannin foams and reference after exposure to 296 K and 65 % relative humidity in a climate chamber.

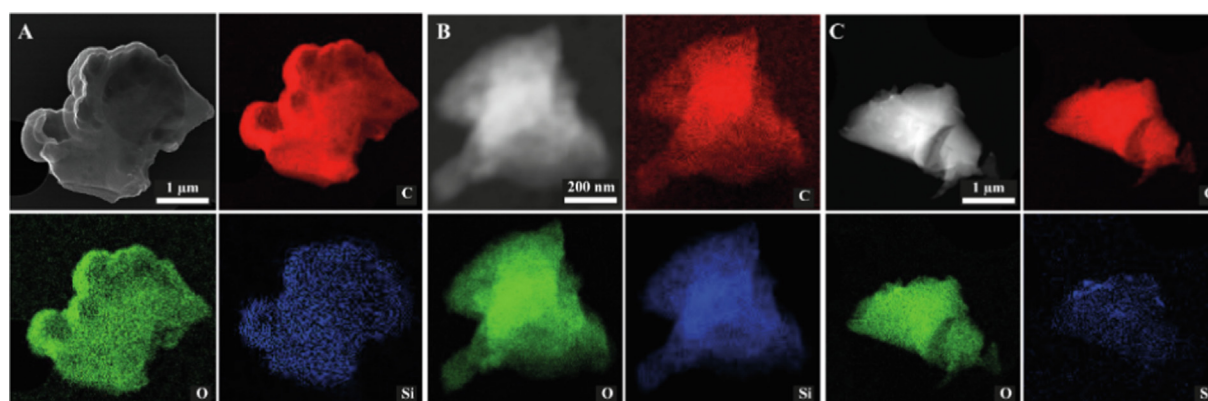


Fig. 8. STEM-EDX of CPTMS<sub>20</sub> (A), MTMS<sub>20</sub> (B) and TMCS<sub>20</sub> (C). Coloring: red–carbon; green–oxygen and blue–silicon.

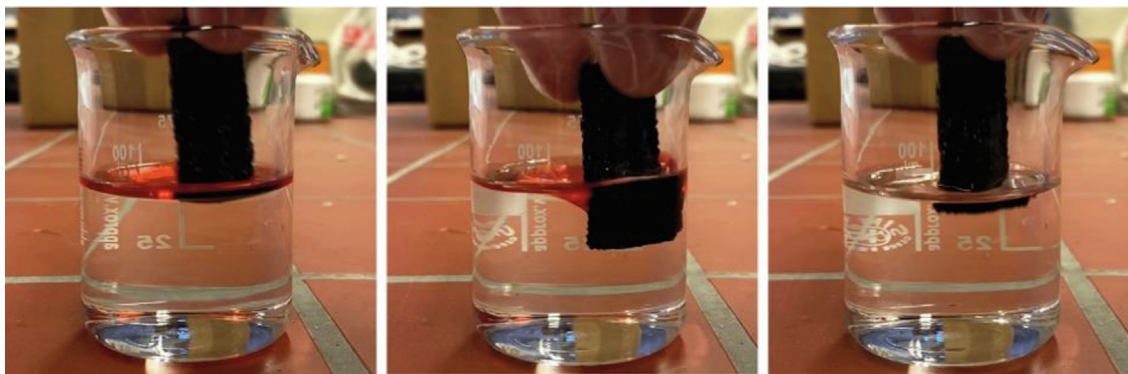


Fig. 10. Absorption of toluene (red) onto the modified foams from a water-toluene mixture.

Using an unmodified tannin-furanic polymer, no absorption of the non-polar contaminant is recorded. Picture series and videos of these experiments can be found in the SI (Fig. S5 – S8).

#### 4. Conclusions

Biogenic tannin-furanic foams present a hydrophilic nature due to the abundant hydroxy groups found in condensed tannins. By using different organosilanes, it is possible to perform silylation reactions with the tannin-furanic polymer, featuring a reversal to hydrophobic behavior. The use of MTMS and CPTMS in heptane at temperatures slightly above ambient allows for a sufficient reaction between the polymer and the alkoxy silane to render the materials hydrophobic with a water contact angle of more than 140°. Due to the three condensable groups, a three-dimensional network is formed with the result of coating the foam polymer's surface. TMCS modification on the other hand takes place at only one site and therefore results in a low weight increase, yet still hydrophobic functionalization of the surface with a contact angle of around 130°. Analytical techniques such as NMR, FT-IR, and TGA show the incorporation of the silane into the biogenic polymer network. The foams' inner surface is completely covered with the silane as indicated by the strongly reduced water vapor absorption and changes in surface morphology visible in SEM. The tannin furanic foam modified with fluorine-free organosilanes shows remarkable reduction in the affinity to water from the surrounding atmosphere, making it an interesting candidate for the application of bio-based insulation material in outdoor areas exposed to alternating thawing/freezing cycles (e.g. insulation boxes or packaging for storage of frozen goods). The small increase in weight does therefore not negatively influence the application in packaging. Furthermore, the water repellent foams allow for designing facade and other directly weathered elements in outdoor applications. As the material has an affinity towards non-polar liquids, it is imaginable to design chromatography columns for the separation of mixtures of non-polar solvents, controlling elution rate by tailoring the surface functionality. Additionally, the material could be used as biogenic sorbent in oil-spills from water after tanker damages like the Exxon-Valdez within a short period of time.

#### CRedit authorship contribution statement

**Thomas Sepperer:** Conceptualization, Methodology, Formal analysis, Investigation, Data curation, Writing – original draft, Visualization, Writing – review & editing. **Alexander Petutschnigg:** Project administration, Supervision, Funding acquisition. **Ann-Kathrin Koopmann:** Investigation. **Jorge Torres-Rodríguez:** Investigation. **Primoz Sket:** Investigation. **Diana E. Bedolla:** Inves-

tigation. **Nicola Hüsing:** Project administration, Supervision, Funding acquisition. **Michael S. Elsaesser:** Conceptualization, Writing – original draft, Writing – review & editing.

#### Data availability

The raw data that support the finding of the study is available from the corresponding authors upon reasonable request.

#### Declaration of Competing Interest

The authors declare that they have no known competing financial interests or personal relationships that could have appeared to influence the work reported in this paper.

#### Acknowledgement

This work was funded by AWS (Austrian Wirtschaftsservice), grant number P1727558-IWB01 in the scope of the EFRE (Europäischer Fonds zur regionalen Entwicklung) Project IWB (Investitionen in Wachstum und Beschäftigung) Zentrum Smart Materials. The Authors acknowledge the support for the NMR analysis, which was the scope of CERIC proposal 20212005. This research was partially funded by the European Regional Development Fund and Interreg V-A Italy Austria 2014–2020 through project ITAT 1059 InCIMA4.

The funding sources did not influence conducting the experiments, interpreting the data, or writing the article.

#### Appendix A. Supplementary material

Supplementary data to this article can be found online at <https://doi.org/10.1016/j.matdes.2023.111936>.

#### References

- [1] C. Lacoste, M.-C. Basso, A. Pizzi, A. Celzard, E. Ella Ebang, N. Gallon, B. Charrier, Pine (P. pinaster) and quebracho (S. lorentzii), tannin-based foams as green acoustic absorbers, *Ind. Crop. Prod.* 67 (2015) 70–73, <https://doi.org/10.1016/j.indcrop.2014.12.018>.
- [2] J. Merle, M. Birot, H. Deleuze, C. Mitterer, H. Carré, F.C. El Bouhtoury, New biobased foams from wood byproducts, *Mater. Des.* 91 (2016) 186–192, <https://doi.org/10.1016/j.matdes.2015.11.076>.
- [3] C. Delgado-Sánchez, F. Santiago-Medina, V. Fierro, A. Pizzi, A. Celzard, Optimisation of “green” tannin-furanic foams for thermal insulation by experimental design, *Mater. Des.* 139 (2018) 7–15, <https://doi.org/10.1016/j.matdes.2017.10.064>.
- [4] J. Sánchez-Martín, J. Beltrán-Heredia, A. Delgado-Regaña, M.A. Rodríguez-González, F. Rubio-Alonso, Adsorbent tannin foams: New and complementary applications in wastewater treatment, *Chem. Eng. J.* 228 (2013) 575–582, <https://doi.org/10.1016/j.cej.2013.05.009>.

- [5] J. Sánchez-Martín, J. Beltrán-Heredia, A. Delgado-Regaña, M.A. Rodríguez-González, F. Rubio-Alonso, Optimization of tannin rigid foam as adsorbents for wastewater treatment, *Ind. Crop. Prod.* 49 (2013) 507–514, <https://doi.org/10.1016/j.indcrop.2013.05.029>.
- [6] G. Tondi, M. Johansson, S. Leijonmarck, S. Trey, Tannin based foams modified to be semi-conductive: Synthesis and characterization, *Prog. Org. Coat.* 78 (2015) 488–493, <https://doi.org/10.1016/j.porgcoat.2014.06.013>.
- [7] Q. Yan, R. Arango, J. Li, Z. Cai, Fabrication and characterization of carbon foams using 100% Kraft lignin, *Mater. Des.* 201 (2021), <https://doi.org/10.1016/j.matdes.2021.109460> 109460.
- [8] A. Pizzi, Tannins medical / pharmacological and related applications: A critical review, *Sustain. Chem. Pharm.* 22 (2021), <https://doi.org/10.1016/j.scp.2021.100481> 100481.
- [9] C. Lacoste, M.C. Basso, A. Pizzi, M.-P. Laborie, A. Celzard, V. Fierro, Pine tannin-based rigid foams: Mechanical and thermal properties, *Ind. Crop. Prod.* 43 (2013) 245–250, <https://doi.org/10.1016/j.indcrop.2012.07.039>.
- [10] G. Riccucci, M. Cazzola, S. Ferraris, V.A. Gobbo, M. Guaita, S. Spriano, Surface functionalization of Ti6Al4V with an extract of polyphenols from red grape pomace, *Mater. Des.* 206 (2021), <https://doi.org/10.1016/j.matdes.2021.109776> 109776.
- [11] A.-K. Koopmann, J. Torres-Rodríguez, M. Salihovic, J. Schoiber, M. Musso, G. Fritz-Popovski, N. Huesing, M.S. Elsaesser, Tannin-based nanoscale carbon spherogels as electrodes for electrochemical applications, *ACS Appl. Nano Mater.* 4 (2021) 14115–14125, <https://doi.org/10.1021/acsnano.1c03431>.
- [12] T. Sepperer, F. Hernandez-Ramos, J. Labidi, G.J. Oostingh, B. Bogner, A. Petutschnigg, G. Tondi, Purification of industrial tannin extract through simple solid-liquid extractions, *Ind. Crop. Prod.* 139 (2019), <https://doi.org/10.1016/j.indcrop.2019.111502> 111502.
- [13] A.L. Missio, B. Tischer, P.S.B. dos Santos, C. Codevilla, C.R. de Menezes, J.S. Barin, C.R. Haselein, J. Labidi, D.A. Gatto, A. Petutschnigg, G. Tondi, Analytical characterization of purified mimosa (*Acacia mearnsii*) industrial tannin extract: Single and sequential fractionation, *Sep. Purif. Technol.* 186 (2017) 218–225, <https://doi.org/10.1016/j.seppur.2017.06.010>.
- [14] A.O. Iroegbu, S.P. Hlangothi, Furfuryl alcohol a versatile, eco-sustainable compound in perspective, *ChemistryAfrica*. 2 (2019) 223–239, <https://doi.org/10.1007/s42250-018-00036-9>.
- [15] G. Tondi, A. Pizzi, Tannin-based rigid foams: Characterization and modification, *Ind. Crop. Prod.* 29 (2009) 356–363, <https://doi.org/10.1016/j.indcrop.2008.07.003>.
- [16] C. Lacoste, M.C. Basso, A. Pizzi, M.P. Laborie, D. Garcia, A. Celzard, Bioresourced pine tannin/furanic foams with glyoxal and glutaraldehyde, *Ind. Crop. Prod.* 45 (2013) 401–405, <https://doi.org/10.1016/j.indcrop.2012.12.032>.
- [17] J. Eckardt, J. Neubauer, T. Sepperer, S. Donato, M. Zanetti, N. Cefarin, L. Vaccari, M. Lippert, M. Wind, T. Schnabel, A. Petutschnigg, G. Tondi, Synthesis and characterization of high-performing sulfur-free tannin foams, *Polymers (Basel)*. 12 (2020) 564, <https://doi.org/10.3390/polym12030564>.
- [18] J. Sánchez-Martín, J. Beltrán-Heredia, C. Carmona-Murillo, Adsorbents from *Schinopsis balansae*: Optimisation of significant variables, *Ind. Crop. Prod.* 33 (2011) 409–417, <https://doi.org/10.1016/j.indcrop.2010.10.038>.
- [19] T. Sepperer, J. Neubauer, J. Eckardt, T. Schnabel, A. Petutschnigg, G. Tondi, Pollutant absorption as a possible end-of-life solution for polyphenolic polymers, *Polymers (Basel)*. 11 (2019), <https://doi.org/10.3390/polym11050911>.
- [20] L. Sommerauer, M.-F. Thevenon, A. Petutschnigg, G. Tondi, Effect of hardening parameters of wood preservatives based on tannin copolymers, *Holzforschung* 73 (2019) 457–467, <https://doi.org/10.1515/hf-2018-0130>.
- [21] T. Sepperer, G. Tondi, A. Petutschnigg, T.M. Young, K. Steiner, Mitigation of ammonia emissions from cattle manure slurry by tannins and tannin-based polymers, *Biomolecules* 10 (2020), <https://doi.org/10.3390/biom10040581>.
- [22] T. Sepperer, A. Petutschnigg, K. Steiner, Long-term study on the nitrogen retention potential of bark extracts and a polymer based thereof in cattle manure slurry, *Bioresour. Technol. Rep.* 18 (2022), <https://doi.org/10.1016/j.biteb.2022.101085> 101085.
- [23] G. Tondi, M. Link, C. Kolbitsch, A. Petutschnigg, Infrared-catalyzed synthesis of tannin-furanic foams, *BioResources* 9 (2013), <https://doi.org/10.15376/biores.9.1.984-993>.
- [24] C. Kolbitsch, M. Link, A. Petutschnigg, S. Wieland, G. Tondi, Microwave produced tannin-furanic foams, *J. Mater. Sci. Res.* 1 (2012), <https://doi.org/10.5539/jmsr.v1n3p84>.
- [25] W. Zhao, A. Pizzi, V. Fierro, G. Du, A. Celzard, Effect of composition and processing parameters on the characteristics of tannin-based rigid foams, Part I: Cell structure, *Mater. Chem. Phys.* 122 (2010) 175–182, <https://doi.org/10.1016/j.matchemphys.2010.02.062>.
- [26] X. Li, A. Pizzi, C. Lacoste, V. Fierro, A. Celzard, Physical properties of tannin/furanic resin foamed with different blowing agents, *BioResources* 8 (2012), <https://doi.org/10.15376/biores.8.1.743-752>.
- [27] M. Jalalian, Q. Jiang, A. Coulon, M. Storb, R. Woodward, A. Bismarck, Mechanically whipped phenolic froths as versatile templates for manufacturing phenolic and carbon foams, *Mater. Des.* 168 (2019), <https://doi.org/10.1016/j.matdes.2019.107658> 107658.
- [28] A. Celzard, M. Stauber, A. Szczurek, V. Fierro, A. Pizzi, A new method for preparing tannin-based foams, *Ind. Crop. Prod.* 54 (2014) 40–53, <https://doi.org/10.1016/j.indcrop.2014.01.012>.
- [29] F.J.J. Santiago-Medina, C. Delgado-Sánchez, M.C.C. Basso, A. Pizzi, V. Fierro, A. Celzard, Mechanically blown wall-projected tannin-based foams, *Ind. Crop. Prod.* 113 (2018) 316–323, <https://doi.org/10.1016/j.indcrop.2018.01.049>.
- [30] T. Sepperer, P. Šket, A. Petutschnigg, N. Hüsing, Tannin-furanic foams formed by mechanical agitation: Influence of surfactant and ingredient ratios, *Polymers (Basel)*. 13 (2021) 3058, <https://doi.org/10.3390/polym13183058>.
- [31] J. Eckardt, T. Sepperer, E. Cesprini, P. Šket, G. Tondi, Comparing condensed and hydrolysable tannins for mechanical foaming of furanic foams: Synthesis and characterization, *Molecules* 28 (2023) 2799, <https://doi.org/10.3390/molecules28062799>.
- [32] W. Zhao, V. Fierro, A. Pizzi, G. Du, A. Celzard, Effect of composition and processing parameters on the characteristics of tannin-based rigid foams Part II: Physical properties, *Mater. Chem. Phys.* 123 (2010) 210–217, <https://doi.org/10.1016/j.matchemphys.2010.03.084>.
- [33] G. Tondi, A. Petutschnigg, Hydrophobic tannin foams, *Int. Wood Prod. J.* 6 (2015) 148–150, <https://doi.org/10.1179/2042645315Y.0000000007>.
- [34] C. Delgado-Sánchez, M. Letellier, V. Fierro, H. Chapuis, C. Gérardin, A. Pizzi, A. Celzard, Hydrophobisation of tannin-based foams by covalent grafting of silanes, *Ind. Crop. Prod.* 92 (2016) 116–126, <https://doi.org/10.1016/j.indcrop.2016.08.002>.
- [35] G. Rangel, H. Chapuis, M.C. Basso, A. Pizzi, C. Delgado-Sanchez, V. Fierro, A. Celzard, C. Gérardin-Charbonnier, Improving water repellence and friability of tannin-furanic foams by oil-grafted flavonoid tannins, *BioResour.* 11 (2016) 7754–7768, <https://doi.org/10.15376/biores.11.3.7754-7768>.
- [36] Z. Shen, S. Kwon, H.L. Lee, M. Toivakka, K. Oh, Cellulose nanofibril/carbon nanotube composite foam-stabilized paraffin phase change material for thermal energy storage and conversion, *Carbohydr. Polym.* 273 (2021), <https://doi.org/10.1016/j.carbpol.2021.118585>.
- [37] S. Yue, X. Li, H. Yu, Z. Tong, Z. Liu, Preparation of high-strength silica aerogels by two-step surface modification via ambient pressure drying, *J. Porous Mater.* 28 (2021) 651–659, <https://doi.org/10.1007/s10934-020-00990-1>.
- [38] B.F. Bergel, L. Leite Araujo, A.L. dos Santos, R.M. da Silva, Campomanes Santana, Effects of silylated starch structure on hydrophobization and mechanical properties of thermoplastic starch foams made from potato starch, *Carbohydr. Polym.* 241 (2020), <https://doi.org/10.1016/j.carbpol.2020.116274> 116274.
- [39] L. Meng, Q. Liu, J. Wang, Z. Fan, X. Wei, Hydrophobic mesoporous silicon dioxide for improving foam stability, *RSC Adv.* 10 (2020) 18565–18571, <https://doi.org/10.1039/D0RA02161J>.
- [40] A. Darmawan, R. Utari, R.E. Saputra, Y. Astuti Suhartana, Synthesis and characterization of hydrophobic silica thin layer derived from methyltrimethoxysilane (MTMS), *IOP Conf. Ser. Mater. Sci. Eng.* 299 (2018), <https://doi.org/10.1088/1757-899X/299/1/012041>.
- [41] E. Ul Haq, S.F.A. Zaidi, M. Zubair, M.R. Abdul Karim, S.K. Padmanabhan, A. Licciulli, Hydrophobic silica aerogel glass-fibre composite with higher strength and thermal insulation based on methyltrimethoxysilane (MTMS) precursor, *Energ. Build.* 151 (2017) 494–500, <https://doi.org/10.1016/j.enbuild.2017.07.003>.
- [42] A. Venkateswara Rao, D. Haranath, Effect of methyltrimethoxysilane as a synthesis component on the hydrophobicity and some physical properties of silica aerogels, *Micropor. Mesopor. Mater.* 30 (1999) 267–273, [https://doi.org/10.1016/S1387-1811\(99\)00037-2](https://doi.org/10.1016/S1387-1811(99)00037-2).
- [43] R.B. Torres, J.P. Varela, A. Lamy-Mendes, L. Durães, Effect of different silylation agents on the properties of ambient pressure dried and supercritically dried vinyl-modified silica aerogels, *J. Supercrit. Fluids* 147 (2019) 81–89, <https://doi.org/10.1016/j.supflu.2019.02.010>.
- [44] F. Henn, R. Tannert, Hydrophobization of monolithic resorcinol-formaldehyde xerogels by means of silylation, *Gels*. 8 (2022) 304, <https://doi.org/10.3390/gels8050304>.
- [45] A. Huang, Q. Liu, N. Wang, X. Tong, B. Huang, M. Wang, J. Caro, Covalent synthesis of dense zeolite LTA membranes on various 3-chloropropyltrimethoxysilane functionalized supports, *J. Memb. Sci.* 437 (2013) 57–64, <https://doi.org/10.1016/j.memsci.2013.02.058>.
- [46] D.K. Owens, R.C. Wendt, Estimation of the surface free energy of polymers, *J. Appl. Polym. Sci.* 13 (1969) 1741–1747, <https://doi.org/10.1002/app.1969.070130815>.
- [47] D.E. Kherroub, M. Belbachir, S. Lamouri, Synthesis of poly(furfuryl alcohol)/montmorillonite nanocomposites by direct in-situ polymerization, *Bull. Mater. Sci.* 38 (2015) 57–63, <https://doi.org/10.1007/s12034-014-0818-3>.
- [48] L. Sommerauer, J. Grzybek, M.S. Elsaesser, A. Benisek, T. Sepperer, E. Dachs, N. Hüsing, A. Petutschnigg, G. Tondi, Furfuryl alcohol and lactic acid blends: Homo- or co-polymerization?, *Polymers (Basel)* 11 (2019), <https://doi.org/10.3390/polym11101533>.
- [49] M. Zanetti, E. Cesprini, M. Marangon, A. Szczurek, G. Tondi, Thermal valorization and elemental composition of industrial tannin extracts, *Fuel* 289 (2021), <https://doi.org/10.1016/j.fuel.2020.119907> 119907.
- [50] K.-Y. Law, Definitions for hydrophilicity, hydrophobicity, and superhydrophobicity: Getting the basics right, *J. Phys. Chem. Lett.* 5 (2014) 686–688, <https://doi.org/10.1021/jz402762h>.
- [51] D. Aslanidou, I. Karapanagiotis, C. Panayiotou, Tuning the wetting properties of siloxane-nanoparticle coatings to induce superhydrophobicity and superoleophobicity for stone protection, *Mater. Des.* 108 (2016) 736–744, <https://doi.org/10.1016/j.matdes.2016.07.014>.
- [52] A.-K. Koopmann, W.J. Malfait, T. Sepperer, N. Huesing, A systematic study on bio-based hybrid aerogels made of tannin and silica, *Materials*. 14 (2021) 5231, <https://doi.org/10.3390/ma14185231>.
- [53] K.-H. Nam, T.-H. Lee, B.-S. Bae, M. Popall, Condensation reaction of 3-(methacryloxypropyl)-trimethoxysilane and diisobutylsilanediol in non-

- hydrolytic sol-gel process, *J. Solgel. Sci. Technol.* 39 (2006) 255–260, <https://doi.org/10.1007/s10971-006-7884-y>.
- [54] Y.-T. Shieh, J.-S. Liao, T.-K. Chen, An investigation of water crosslinking reactions of silane-grafted LDPE, *J. Appl. Polym. Sci.* 81 (2001) 186–196, <https://doi.org/10.1002/app.1428>.
- [55] C. Jiao, Z. Wang, Z. Gui, Y. Hu, Silane grafting and crosslinking of ethylene-octene copolymer, *Eur. Polym. J.* 41 (2005) 1204–1211, <https://doi.org/10.1016/j.eurpolymj.2004.12.008>.
- [56] Y.-T. Shieh, C.-M. Liu, Silane Grafting Reactions of LDPE, HDPE, and LLDPE, 1999, doi: 10.1002/(SICI)1097-4628(19991227)74:14.
- [57] Wärmedämmstoffe aus Polyurethan-Hartschaum Herstellung-Anwendung-Eigenschaften, 2008, [www.daemmt-besser.de](http://www.daemmt-besser.de) (accessed July 19, 2022).
- [58] Wasseraufnahme von Polystyrol-Dämmstoff EPS | Bau SV - Sachverständige für Schäden an Gebäuden & Bauphysik, (n.d.). <https://www.bau-sv.de/wasseraufnahme-von-polystyrol-daemmstoff-eps/> (accessed July 19, 2022).